



HAL
open science

An Enhanced Receiver to Decode Superposed LoRa-like Signals

Mohamed Amine Ben Temim, Guillaume Ferré, Baptiste Laporte-Fauret,
Dominique Dallet, Bryce Minger, Loïc Fuché -

► **To cite this version:**

Mohamed Amine Ben Temim, Guillaume Ferré, Baptiste Laporte-Fauret, Dominique Dallet, Bryce Minger, et al.. An Enhanced Receiver to Decode Superposed LoRa-like Signals. IEEE Internet of Things Journal, 2020, 7 (8), pp.7419 - 7431. 10.1109/JIOT.2020.2986164 . hal-02566683

HAL Id: hal-02566683

<https://hal.science/hal-02566683>

Submitted on 11 May 2021

HAL is a multi-disciplinary open access archive for the deposit and dissemination of scientific research documents, whether they are published or not. The documents may come from teaching and research institutions in France or abroad, or from public or private research centers.

L'archive ouverte pluridisciplinaire **HAL**, est destinée au dépôt et à la diffusion de documents scientifiques de niveau recherche, publiés ou non, émanant des établissements d'enseignement et de recherche français ou étrangers, des laboratoires publics ou privés.

An Enhanced Receiver to Decode Superposed LoRa-like Signals

¹Mohamed Amine BEN TEMIM, *Student Member, IEEE*, ¹Guillaume FERRÉ, *Member, IEEE*, ^{1,2}Baptiste LAPORTE-FAURET, *Student Member, IEEE*, ¹Dominique DALLET, *Member, IEEE*, ²Bryce MINGER and ²Loïc FUCHÉ

¹Univ. Bordeaux, CNRS, Bordeaux INP, IMS, UMR 5218, F-33400, Talence, France
²THALES, France

Email: forename.name@{¹ims-bordeaux.fr, ²thalesgroup.com}

Abstract—To cope with the exponential rise of emerging technology, there have been significant developments in intelligent communication systems aimed at low power and long-range wireless Internet of Things (IoT) communication. Among the various number of leading low power wide area network (LPWAN) technologies, Long Range (LoRa) has emerged to be an attractive solution to connect devices in free bands. Operating in unlicensed bands requires connected objects to reduce their energy consumption. To this end, one of the adopted techniques is the random access to the radio channel, which leads to an increase in the probability of packet collisions. In this paper, we propose a new receiver capable to decode several IoT LoRa-Like signals simultaneously received with the same Spreading Factor which leads to destructive collisions. Based on the particular structure of the received signals and the Successive Interference Cancellation (SIC) algorithm, we propose a novel approach to decode superposed LoRa-like signals iteratively. Simulations and real LoRa deployments are presented to validate the efficiency of our receiver.

Index Terms—LoRa, IoT, Synchronization, SIC, Collisions

I. INTRODUCTION

THE deployment of Internet of Things (IoT) involves many new challenge. Among them, energy consumption is paramount either from the economic than the ecological perspective. Indeed, according to IoT analytics study [1] the number of active IoT devices is expected to grow to 10 billion by 2020 and 22 billion by 2025. According to the same study more than 2 billion devices will be connected through low power wide area networks (LPWAN) by 2025.

If the predictions of the exponential increase in the number of connected objects are confirmed, their density in urban areas will lead to a saturation of the electromagnetic spectrum in the free bands. Indeed, operating in free bandwidth, typically industrial, scientific, and medical (ISM) bands, offers the possibility to different devices to access the spectrum and provide wide number of services as long they abide by regulations. The primary advantage is license cost effectiveness. Nevertheless, the main downside of uncontrolled channel access are packet collisions.

Copyright (c) 2020 IEEE. Personal use of this material is permitted. However, permission to use this material for any other purposes must be obtained from the IEEE by sending a request to pubs-permissions@ieee.org.

Many technologies are specifically designed to connect various objects to the internet. Among them, LoRa [2] has emerged to be an interesting solution. LoRa technology was developed by a french company called Cycleo, and then acquired and patented by Semtech [2] which is at present selling LoRa chips. As explained in [3], [4], LoRa is a spread spectrum technology and more precisely, it is the Chirp Spread Spectrum (CSS) modulation [5] that is used to transmit binary information. This modulation technique requires the use of various spreading factors (SFs) to obtain orthogonal transmissions and reduce destructive collisions. In such configuration, destructive collisions occur only when two or more signals are simultaneously received in the same frequency band and with the same SF . Packet collisions are unavoidable in communication systems with random access to the channel such as LoRa-based networks. Yet, the processing of the latter collisions can be preventive or palliative. Among preventive approaches, we can mention the use of random-access channel (RACH) in LoRaWAN [6]. In such configuration, if the nodes do not receive an acknowledgment, due to an out of range communication or the presence of interfering signals, they wait for random period before transmitting again at the expense of the spectral efficiency. In the same context, authors in [7] propose to reduce the occurrence of destructive collisions in LoRaWAN by using redundant gateways. However, in this work, we propose a palliative approach at the physical layer level. This processing allows to reduce the number of re-transmitted packets which will enhance the spectral efficiency.

In this paper, we deal with an uplink communication case where several LoRa-like signals are simultaneously received over the same channel and with the same SF at the gateway. Due to the random access protocols adopted by LoRa-based networks and the deployment of low-cost crystal oscillators which have an inherent mismatch with their nominal frequency, all the received signals are randomly desynchronized in time and suffer from carrier frequency offsets. The goal of this paper is to design an efficient receiver capable to decode superposed LoRa-like signals in such configuration. Our approach is based on the Successive Interference Cancellation (SIC) algorithm which is relevant because the interference can be removed efficiently based on the symbol estimation. The

proposed algorithms are implemented at the gateway, which has generally no restriction on power consumption since it is continuously supplied¹. This processing would reduce the energy consumption of the nodes and enhance their spectral efficiency since it decreases the number of re-transmitted packets. Finally, to evaluate the performance of our receiver, we perform simulation using LoRa-like signals synthesized with Matlab® before considering real LoRa deployments.

This paper is organized as follows. In section II, the related works are presented. Section III details the models of transmitted and received LoRa-like signals. Section IV presents our proposed algorithms to enhance the reception while section V highlights the efficiency of the proposed approach on different simulations and real data results. Finally, section VI presents conclusions and future prospects.

II. RELATED WORKS

In this section, we review existing works related to our paper in order to highlight our contribution to face the problem of same- SF interference in LoRa.

Authors in [8], [9] have analyzed the impact of a same- SF interfering signal on the decoding performance of the signal of interest by presenting the theoretical models of the interference. This analysis is done at the expense of the interfering signal whose information is lost. This paper does not propose any method to process the interference issue and thus decoding the colliding signals.

Simulators to evaluate the impact of same and different SF interference on LoRaWAN performance are implemented in [10], [11]. The authors showed that different SF are not perfectly orthogonal and such collision can lead to a packet loss if the Signal to Interference Ratio (SIR) is lower than a threshold value for each SF configuration. Moreover, for same- SF collisions and by using the capture effect, they assumed that the signal of interest is well decoded if its power is 6 dB greater than the total power of the interfering signals. These papers allow us to know the limits of our method but in no way propose solutions to treat interference as we suggest in this paper.

In a similar context, authors in [12] studied the capture effect (i.e. define the SIR threshold allowing the accurate decoding of the signal of interest) and proposed to use SIC algorithm to decode the superposed signals. However, this analysis does not provide any explanation about how the interference cancellation and the synchronization are performed. They presented the throughput of the proposed system using an abstraction of the physical layer since they assumed that the SIC is well performed if the SIR is greater than a threshold value.

A novel approach to decode non-orthogonal LoRa signals using the specific structure of the chirps is presented in [13]. However, their proposed algorithms could decode only two superposed signals and require the receiver to be perfectly synchronized or slightly desynchronized which is unrealistic in a random access scenario as adopted by LoRa-based networks.

¹It should be noted that without power consumption constraints, the proposed algorithms can also be implemented on the nodes.

In addition, using the spectrogram² of the chirps to decode the superposed signals is not very efficient since it requires a good Signal to Noise Ratio (SNR) to identify them. And basically the problems occur when we are closed to the receiver sensitivity.

Finally, we already dealt in [14] with an uplink case where two desynchronized LoRa-like signals are simultaneously received in the same channel and with the same SF . We proposed an approach based on the Fast Fourier Transform (FFT) representation to decode both signals. However, we assumed that the signal having the highest power was received first which is not always the case. Our contribution in this paper can be viewed as a generalization of this work.

Based on this, to the best of our knowledge, there is no work that deals with same- SF interference by considering almost a real world scenario (i.e. random time and frequency desynchronization). Indeed, we provide mathematical models allowing us to develop our novel approach to face this interference issue. Furthermore, using a simple implemented SIC algorithm makes our work easily testable in the current LoRa chip which we have proved in section V-B.

We propose the following Table to summarize this state of the art:

TABLE I: Related works comparison

Papers \ KPI	Frequency synchronization algorithm	Time synchronization algorithm	Interference cancellation algorithm	Decoding performance algorithm
[8], [9]	✗	✗	✗	Only the strongest signal
[10], [11]	✗	✗	✗	Only the strongest signal
[12]	✗	✗	✓	Not precised
[13]	✗	✗	✗	Only 2 superposed signals
[14]	✗	✓	✓	Only 2 superposed signals
Our paper	✓	✓	✓	All superposed signals

III. SYSTEM MODEL

We consider an uplink communication system where several LoRa-like signals are supposed to be simultaneously received on the same channel and with the same SF . Indeed, those signals come from IoT LoRa nodes transmitting data to a gateway as depicted in Fig. 1. As presented in [15], receiving simultaneously two or more signals with the same SF leads to a loss of orthogonality and may cause the loss of all packets.

In the remaining of this paper, we consider the following notations and definitions:

²A spectrogram is a visual representation of the spectrum of frequencies of a signal as it varies with time.

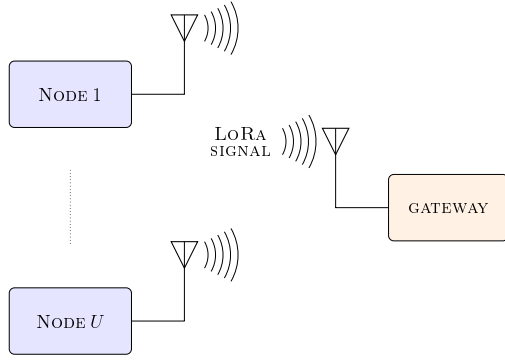


Fig. 1: Test-bed for U LoRa transmissions simultaneously received by the gateway.

TABLE II: Notations and Definitions

Notations	Definitions
T	symbol time
$M = 2^{SF}$	total symbol number
$B = \frac{2^{SF}}{T}$	signal bandwidth
$f(t) = \frac{B}{T}t, \forall t \in [-\frac{T}{2}, \frac{T}{2})$	raw chirp
T_s	sampling time
U	number of superposed signals
$\mathbb{1}_{[0,x)}(t)$	the indicator function
$x \bmod M$	the modulo M operation of x
$\lfloor \cdot \rfloor / \lceil \cdot \rceil$	flooring/rounding operation

A. Presentation of the transmitted LoRa signals

In this section, we present the structure of the signals transmitted by LoRa nodes. For more details on the LoRa physical layer, reader can refer to [9], [15], [16].

1) *LoRa PHY layer principle*: As we mentioned, LoRa is a spread spectrum technology derived from the CSS modulation. Indeed, for each node $i \in \{1, \dots, U\}$, we define $f_i(t - pT)$ as the transmitted chirp $\forall t \in [pT - \frac{T}{2}, pT + \frac{T}{2}]$. This chirp is obtained using $\gamma_i(p) = \frac{m_i(p)}{B}$ and performing a cyclic shift as depicted by Fig. 2. It should be noted that $m_i(p)$ corresponds to the transmitted symbol at time pT . It is a random value uniformly distributed in $\llbracket 0, M - 1 \rrbracket$ and is obtained from the binary to decimal conversion of SF bits.

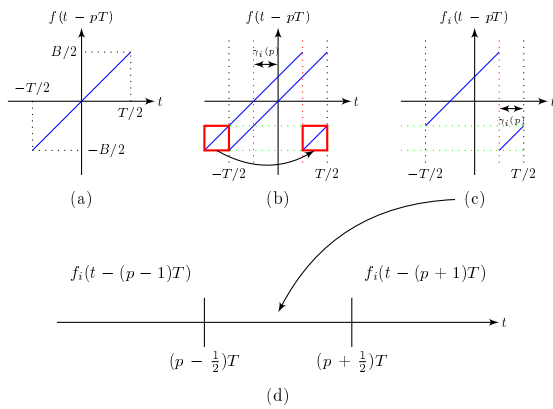


Fig. 2: Symbol \rightarrow chirp association process - (a) up raw chirp - (b) process principle - (c) associated chirp - (d) temporal location of the chirp.

$f_i(t - pT)$ can be expressed as the derivative of its phase $\phi_i(t - pT)$:

$$f_i(t - pT) = \frac{1}{2\pi} \frac{d\phi_i(t - pT)}{dt} \quad (1)$$

Thus, we obtain for $t \in [pT - \frac{T}{2}, pT + \frac{T}{2} - \gamma_i(p)]$:

$$\phi_i(t - pT) = 2\pi \left[\frac{B}{2T}t^2 + \frac{m_i(p)}{T}t \right] \quad (2)$$

And for $t \in [pT + \frac{T}{2} - \gamma_i(p), pT + \frac{T}{2}]$:

$$\phi_i(t - pT) = 2\pi \left[\frac{B}{2T}t^2 + \left(\frac{m_i(p)}{T} - B \right) t \right] \quad (3)$$

If we note $x_i(t)$ the complex envelope of the signal transmitted by the i^{th} LoRa node, we have:

$$x_i(t) = \sum_{p \in \mathbb{Z}} e^{j\phi_i(t-pT)} \quad (4)$$

After giving a brief overview of the LoRa physical layer and its CSS modulation, we dedicate the next paragraph to detail the LoRa frame structure.

2) *LoRa frame structure*: As defined in [17], the LoRa frame is composed of:

- A preamble with a number N_p of up raw chirp symbols which is exploited to detect the presence of LoRa signal [18].
- A word of synchronization called a “sync word” which is constituted of 2 special modulated symbols [19]. It is used for the timing frame synchronization to convey the end of the preamble to the receiver and thus, to know the effective start of the frame³.
- A Start of the Frame Delimiter (SFD) which is composed of 2.25 down-chirps that could be used for the frequency synchronization.
- A PHY-header containing the frame information, a variable-length PHY-payload and a cyclic redundancy check (CRC).

As highlighted in [17], the PHY-header and the CRC are optional. The previous structure of a LoRa frame is illustrated in Fig. 3, which is obtained by recording real LoRa data using our own-made nodes as we will present in section V-B.

3) *LoRa frame generation*: The signal transmitted by each LoRa node is started by the aforementioned preamble, the sync word and the SFD. Then, its stream of data is generated in form of N_s^i symbols that are uniformly distributed in $\llbracket 0, M - 1 \rrbracket$.

Based on the LoRa frame structure, a realistic complex envelope of the signal transmitted by the i^{th} node can be written as:

$$s_i(t) = \sum_{p=0}^{N_p-1} e^{j\phi(t-pT)} + \sum_{p=N_p}^{N_p+1} e^{j\tilde{\phi}_p(t-pT)} + \sum_{p=N_p+2}^{N_t} e^{-j\phi(t-pT)} + \sum_{p=N_t+1}^{N_s^i+N_t-1} e^{j\tilde{\phi}_p^i(t-pT)} \quad (5)$$

³It also can be used to distinguish between devices from different networks. Indeed, if the sync word of the received packet does not match with the one configured in the gateway, then the gateway will stop receiving this packet.

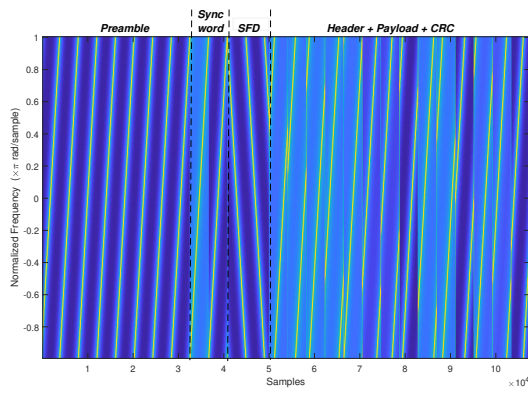


Fig. 3: Spectrogram of the LoRa frame obtained by recording real LoRa data.

where $N_t = N_p + 4.25$ is the total number of symbols of the preamble, synch word and SFD and $\tilde{\phi}_p(t - pT)$ (resp. $\phi(t) = 2\pi \frac{B}{2T} t^2$), $t \in [pT - \frac{T}{2}, pT + \frac{T}{2}]$, is the instantaneous phase corresponding to a specific modulated symbols of the sync word (resp. raw chirp).

B. Received signals at the gateway

In this section, we detail the mathematical models and the demodulation principle of the received signals at a LoRa gateway. Due to the complete lack of synchronization between the gateway and the nodes, the continuous-time version of the received signal, when several LoRa-like frames with the same *SF* are superposed, can be written as:

$$y(t) = \sum_{i=1}^U \sqrt{P_i} s_i(t - \Delta t_i) e^{-j(2\pi \Delta f_i t - \theta_i)} + w(t) \quad (6)$$

where P_i , θ_i , Δt_i and Δf_i are the power, the initial phase, the time desynchronization and the frequency offset of the i^{th} received signal respectively and $w(t)$ is the complex Additive White Gaussian Noise (AWGN) signal with σ_w^2 its variance.

We consider at first a reception case of one signal without any interference to explore the LoRa demodulation principle and then interfering signals are analyzed. We point out that all the processing is done at the gateway using the discrete version of the received signals and time and frequency synchronizations are needed before decoding their information.

1) *Case without interference* ($U = 1$): Similar to any other modulation mechanism, the decoding process of LoRa-like signals requires an accurate time and frequency synchronizations. Hence, the received signal synchronized on Node 1 frame and sampled at $T_s = \frac{1}{B}$ is given by:

$$y(n) = \sqrt{P_1} s_1(n) + w(n) \quad (7)$$

with $w(n)$ being the discrete-time version of the noise.

The transmitted symbols are detected by multiplying each T -long section of the received signal by complex envelope corresponding to the conjugate of the raw chirp (i.e. down-chirp signal). Based on the principle of the LoRa-Like symbol detection detailed in [17], [20] and Fig. 4, the signal obtained

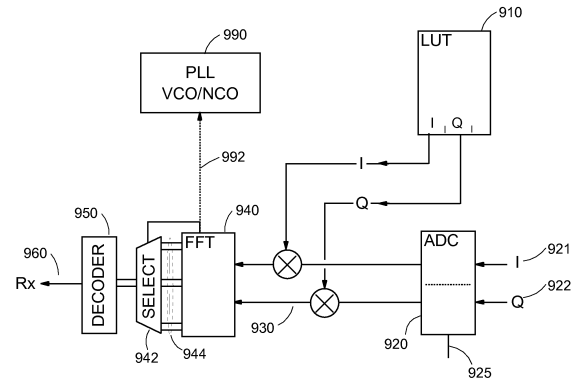


Fig. 4: LoRa receiver architecture [20, Fig. 9].

after the FFT processing of p^{th} symbol of node 1 without any interfering signals, can be expressed as:

$$Y(k, p) = \frac{1}{\sqrt{M}} \sum_{n=0}^{M-1} y(nT_s + pT) e^{-j\phi(nT_s + pT)} e^{-j2\pi \frac{nk}{M}} \quad (8)$$

with $k \in \llbracket 0, M-1 \rrbracket$, thus based on [15] and after some calculations:

$$Y(k, p) = \sqrt{P_1 M} \delta(k - m_1(p)) + W(k, p) \quad (9)$$

where $\delta(k)$ represents the Kronecker impulse and $W(k, p) \sim \mathcal{N}_{\mathbb{C}}(0, \sigma_w^2)$ is the FFT of the noise.

The estimation of the symbol $m_1(p)$ is done by looking for the frequency k that maximizes the module of (9).

2) *Case of superposed signals* ($U > 1$): To detect, synchronize and decode LoRa-like signals, the gateway has to be in a listening status. To this end, the received signals are sampled and multiplied by a train of down-chirp signals. It should be noted that this step is called the de-chirping operation in the literature [21]. Indeed, the multiplication by the de-chirping sequence is performed, not necessarily in a synchronized mode at first since the the beginning instant of each packet is not known in advance by the receiver. A practical method to perform accurate time and frequency synchronizations of the received signals is proposed in section IV.

Based on Fig. 5, the de-chirping sequence, sampled at T_s , can be expressed as:

$$d(n) = \sum_{p \in \mathbb{Z}} e^{-j\phi(nT_s - pT)} \quad (10)$$

As the processing of LoRa-like signals at the gateway is done after the Analog to Digital Converter (ADC), the discrete-time version of the received signal sampled at T_s is given by:

$$y(n) = \sum_{i=1}^U \sqrt{P_i} s_i(n - \Delta n_i) e^{-j(2\pi \Delta f_i n T_s - \theta_i)} + w(n) \quad (11)$$

The discrete time shift Δn_i between the beginning of the de-chirping sequence and each superposed LoRa signal is expressed as: $\Delta n_i = \frac{\Delta t_i}{T_s} = K_i M + \tau_i$ with $K_i \in \mathbb{N}$ and τ_i denoting the relative time offset between the i^{th} signal with the de-chirping sequence and following the uniform distribution

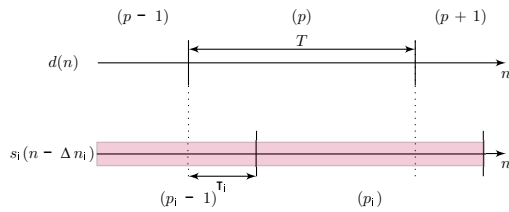


Fig. 5: LoRa-Like symbol detection principle.

$\mathcal{U}[0, M)$. τ_i can not be constrained to an integer value, since supposing that the de-chirping sequence is sample-aligned with the received signals is not realistic. Therefore, this time-offset is given by: $\tau_i = \lfloor \tau_i \rfloor + \epsilon_i$, $\epsilon_i \in [0, 1)$.

Based on the principle of the LoRa-Like symbol detection detailed in [9], [15], [17] and on Fig. 5, the signal obtained after the FFT, which corresponds to the processing of p^{th} T -long section of the de-chirping sequence is equal to:

$$Y(k, p) = \frac{1}{\sqrt{M}} \sum_{n=0}^{M-1} \underbrace{(y(n, p)d(n, p))}_{z(n, p)} e^{-j2\pi \frac{nk}{M}} \quad (12)$$

where $y(n, p) = y(n)$ and $d(n, p) = d(n) \forall n \in \llbracket pM, (p+1)M - 1 \rrbracket$. Thus based on [15], [22], Fig. 5 and after some calculations we obtain:

$$\begin{aligned} z(n, p) &= \sum_{i=1}^{U_p} z_{\tau_i}(n, p) + w(n) \\ &= \sum_{i=1}^{U_p} (\sqrt{P_i} e^{j(2\pi n \frac{\bar{m}_i(p_i-1)}{M} + \phi^{p_i-1})} \mathbb{1}_{\llbracket 0, \lfloor \tau_i \rfloor \rrbracket}(n) \\ &\quad + \sqrt{P_i} e^{j(2\pi n \frac{\bar{m}_i(p_i)}{M} + \phi^{p_i})} \mathbb{1}_{\llbracket \lfloor \tau_i \rfloor + 1, M-1 \rrbracket}(n)) \\ &\quad + w(n) \end{aligned} \quad (13)$$

where

- $U_p \in \{1, \dots, U\}$ is the number of received signals in the p^{th} T -long section of the de-chirping sequence,
- ϕ^{p_i} , $p_i \in \{1, \dots, N_t + N_s^i\}$, is the initial phase of the i^{th} received signal in its p_i^{th} T -long section,
- $\bar{m}_i(p_i)$, $p_i \in \{1, \dots, N_t + N_s^i\}$, is the frequency of the detected peak of latter signal in a non synchronized mode. The relation between $\bar{m}_i(p_i)$ and the symbol initially transmitted is expressed as:

$$\bar{m}_i(p_i) = m_i(p_i) - \lfloor \tau_i \rfloor - \lfloor \Delta f_i T \rfloor \pmod{M} \quad (14)$$

Based on the structure of i^{th} de-chirped signal $\forall i \in \{1, \dots, U\}$, we can observe that the FFT of a non synchronized signal gives two cardinal sines. Here, we notice that the maximum number of peaks that could be detected is $2 \times U_p$ depending on the positions of the latter peaks (probability of 2 superposed peaks) and the noise level of each signal. Therefore, in a non synchronized mode, an accurate decoding of these signals is impossible.

In the next section, we propose a novel approach to detect, synchronize and decode the maximum number of non-orthogonal signals simultaneously received.

IV. PROPOSED ALGORITHMS TO PROCESS THE RECEPTION OF MULTIPLE NON-ORTHOGONAL LoRa-LIKE SIGNALS

In this section, we propose to design an enhanced receiver able to synchronize and decode simultaneously received non-orthogonal LoRa-like signals. Our approach consists in processing LoRa signals in a given time window. Indeed, the receiver sets a constant block duration T_B and tries to iteratively decode the maximum number of signals received along this duration. The principle consists in:

- detecting the received signals and identifying the strongest one,
- decoding the strongest signal information,
- reproducing its complex envelope and removing it from the received signal (SIC algorithm).

The latter operations are repeated until there is no detected LoRa-like signal left. We point out that each two consecutive blocks are overlapped by at least a maximum packet duration⁴ to ensure the processing of all the received signals information.

A. Strongest signal synchronization algorithms

Our algorithms aim to detect the effective start of the s^{th} received signal, which corresponds to the strongest signal, and to compensate its frequency offset Δf_s . To this end, we propose a coarse and a fine synchronization.

1) Coarse synchronization based on preamble detection:

The detection of the presence of LoRa-like signals is performed by a gateway in a listening mode. This is done by continuously de-chirping the sampled received signals. After that, a FFT is processed in each T -long section as presented in (12). Based on (13), the contributions of a LoRa-like signal in a T -long section, for different desynchronization scenarios, are given in Table III.

TABLE III: Time and frequency desynchronizations impacts on FFT representation of the symbol to estimate

Synchronization	Observations after the FFT processing
$\tau_i \neq 0, \Delta f_i = 0$	Two cardinal sines shifted by τ_i
$\tau_i = 0, \Delta f_i \neq 0$	One cardinal sine shifted by $\Delta f_i T$
$\tau_i \neq 0, \Delta f_i \neq 0$	Two cardinal sines shifted by $\tau_i + \Delta f_i T$

Nevertheless, given that all the symbols of LoRa preamble are equal to zero. Thus, only one peak is detected even in a non synchronized mode (time and frequency desynchronizations) since the contribution of two consecutive zero symbols would be superposed in same FFT bin as depicted in Fig. 6 for the strongest signal. Thereby, given that $\forall p_s \in \{1, \dots, N_p\}$, $m_s(p_s) = 0$ and by using (14), a nearly accurate estimation of the total shift of the main peak $\hat{\tau}'_s = \tau_s + \Delta f_s T$ can be easily performed.

Given the structure of LoRa packet preamble, averaging the module squared of the FFTs over each N_p T -long sections would increase the certainty of preamble detection. If we note

⁴As an example, in LoRaWAN, the maximum packet duration is known for each SF .

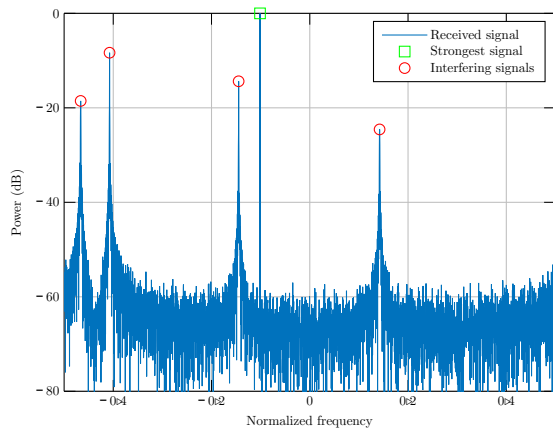


Fig. 6: Result of the FFT processing when the preamble of the strongest signal is superimposed with two interfering signals ($U_p = 3$).

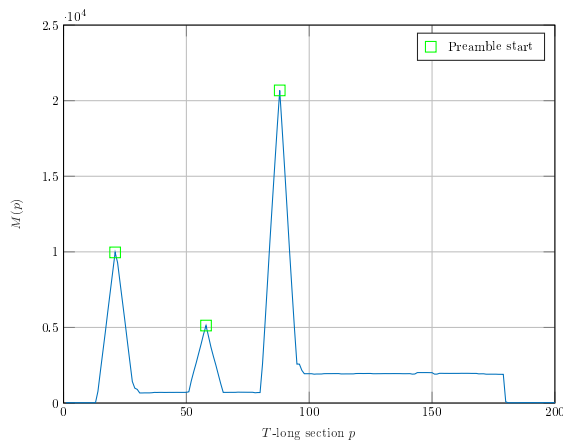


Fig. 7: Preamble detection process ($U = 3$).

$T(k, p)$, $k \in \llbracket 0, M - 1 \rrbracket$, $p \in \{1, \dots, N_B\}$ and $N_B = \lfloor \frac{T_B}{T} \rfloor$, the averaging function, we have:

$$T(k, p) = \sum_{j=p}^{p+N_p-1} \left| \frac{Y(k, j)}{\sigma_w} \right|^2 \quad (15)$$

It should be noted that the estimation of the AWGN variance σ_w^2 is done on silent periods when no signal is received. To coarsely estimate the index \hat{K}_s of the T -long section that corresponds to the beginning of the strongest signal preamble, we compute the function $M(p)$, as presented in Fig. 7 when three signals are simultaneously received. This function represents the maximum value of $T(k, p)$, $\forall p \in \{1, \dots, N_B\}$.

$$M(p) = \max_k (T(k, p)). \quad (16)$$

Then, if we note \hat{K}_s an estimation of K_s we have:

$$\hat{K}_s = \underset{p}{\operatorname{argmax}} (M(p)). \quad (17)$$

We notice that, in each iteration of our algorithm, the identification of the maximum of $M(p)$ requires the definition of a threshold value to detect the existence of LoRa-like signals in the data block. This value is set using a classical hypothesis test on $T(k, p)$ according to the noise level.

knowing that the FFT of the noise in p^{th} T -long section $W(k, p)$, $k \in \llbracket 0, M - 1 \rrbracket$, follows the Normal distribution $\mathcal{N}_{\mathbb{C}}(0, \sigma_w^2)$. Thus, it is easy to demonstrate that $\sum_{j=p}^{p+N_p-1} \left| \frac{W(k, j)}{\sigma_w} \right|^2$ follows the chi-squared distribution $\chi^2(\cdot; N_p)$ with N_p is the degree of freedom.

If we note P_{fa} the probability of the false alarm and we define hypothesis tests

- $\mathcal{H}_0: \{U_j = 0, \forall j \in \{p, \dots, p + N_p\}\}$,
- $\mathcal{H}_1: \{\exists j \in \{p, \dots, p + N_p\}, U_j \neq 0\}$,

we have:

$$\begin{aligned} P_{fa} &= P[\mathcal{H}_1/\mathcal{H}_0] \\ &= P[T(k, p) > Th/T(k, p) \sim \chi^2(\cdot; N_p)] \\ &= 1 - P[T(k, p) < Th/T(k, p) \sim \chi^2(\cdot; N_p)] \\ &= 1 - F_{\chi^2}(Th; N_p) \end{aligned} \quad (18)$$

where $F_{\chi^2}(\cdot; N_p)$ is the cumulative density function of the chi-squared distribution with N_p degree of freedom.

Thus, the threshold Th could be expressed as:

$$Th = F_{\chi^2}^{-1}(1 - P_{fa}; N_p) \quad (19)$$

Therefore, if $T(k, p) < Th, \forall p \in \{1, \dots, N_B\}$, no LoRa-like signal is detected in the considered block.

2) *Fine synchronization based on the SFD*: The previous synchronization procedure has enabled the detection of the strongest received signal and the estimation of K_s and τ'_s . However, due to the random distribution of the total shift τ'_s (caused by τ_s and Δf_s), we will have a significant uncertainty on the estimation of K_s . Furthermore, to estimate the time shift τ_s it is mandatory to compensate the frequency shift. As a consequence, we propose a fine frame synchronization procedure in order to reduce the latter uncertainty and to compensate the frequency offset Δf_s .

To same end, authors in [21] use a local correlation with the preamble and the sync word whereas authors in [23] propose to perform a framing of the SFD by increasing the time-based FFT resolution. Here, we suggest an optimized method based also on the SFD framing. It is simply needed to compensate the total shift $\hat{\tau}'_s$ and apply an up-chirp sequence to the T -long sections where the down-chirp symbols of the SFD are expected. The two highest successive FFTs maxima in the same FFT bin indicate the beginning of the down-chirps. Hence, an accurate estimation of K_s can be performed.

After the latter up-chirping operation the SFD down-chirp symbols must be decoded with a zero value in the case of accurate time and frequency synchronizations. However, due to the frequency offset the latter symbols are shifted as depicted in (14) and in Table III.

If we note \hat{m}'_s and \bar{m}'_s the detected FFT argmax of a down-chirp symbol after and before compensating $\hat{\tau}'_s$ respectively and m_s the transmitted down-chirp symbol, we have:

$$\begin{aligned} \hat{m}'_s &= \bar{m}'_s - \hat{\tau}'_s \quad \text{mod } M \\ &= m_s + \tau_s - \Delta f_s T - \tau_s - \Delta f_s T \quad \text{mod } M \\ &= m_s - 2\Delta f_s T \quad \text{mod } M \end{aligned} \quad (20)$$

Given that $m_s = 0$ and by estimating the down-chirp symbols after compensating $\hat{\tau}'_s$, we can easily deduce the frequency

offset Δf_s and compensate it. However, this estimation is biased since the latter offset can not be constrained to an integer value. Therefore, an interpolation is performed around the FFT maximum sample to refine the search.

Finally, after the estimation of τ'_s and Δf_s , the time offset $\hat{\tau}_s$ could be easily deduced.

B. Decoding the strongest signal

Once the receiver is synchronized to the beginning of the frame of the signal having the highest received power, a synchronized de-chirping process is applied to it. Consequently, a FFT is performed for each T -long section of the latter frame.

If we note $z_s(n, p_s)$ the de-chirped received signal synchronized on the strongest signal, we have:

$$z_s(n, p_s) = \sqrt{P_s} e^{j(2\pi n \frac{m_s(p_s)}{M} + \phi^{p_s})} + \sum_{i=1}^{U_{p_s}-1} z_{\tau_i^s}(n, p_s) + w(n) \quad (21)$$

with $n \in [\Delta n_s + p_s M, \Delta n_s + (p_s + 1)M - 1]$ and τ_i^s being the time offset between the synchronized signal and the i^{th} interfering signal. Using (12) and some calculation, the FFT of $z_s(n, p_s)$ can be expressed as:

$$Y_s(k, p_s) = \sqrt{P_s M} \delta(k - m_s(p_s)) + \sum_{i=1}^{U_{p_s}-1} Y_i(k, p_s) + W(k) \quad (22)$$

where $Y_i(k, p_s)$ is the FFT of i^{th} signal interfering the decision of the p_s^{th} symbol. Hence, the estimation of the p_s^{th} transmitted symbol is obtained as:

$$\hat{m}_s(p_s) = \underset{k}{\operatorname{argmax}}(|Y^s(k, p_s)|) \quad (23)$$

In this context, several works have evaluated LoRa-like signal decoding performance. Authors in [8], [9] presented the Bit Error Rate (BER) curves of LoRa signals (with and without same- SF interference) as function of the Signal to Noise Ratio (SNR). The later is equal to $\frac{P}{\sigma_w^2}$ where P represents the power of the received signal. Then, [8] demonstrated that the SNR thresholds $\Gamma_{th}^{(SF)}$, necessary to guarantee the coverage characterized by LoRa network without interference, are those associated to a BER of 10^{-5} . The values of these SNR thresholds are given in Table IV.

TABLE IV: SNR thresholds for LoRa-Like signal with $B = 125\text{KHz}$

SF	7	8	9	10	11	12
$\Gamma_{th}^{(SF)}$ (dB)	-6	-9	-12	-15	-17.5	-20

They showed also that the SNR thresholds are affected in the presence of a same- SF interference and proved that the decoding performance of the signal of interest is slightly affected if its power is at least 6 dB greater than the power of the interfering signal.

C. Strongest signal cancellation

Once the receiver is synchronized on the strongest signal, it estimates the frequency as presented in (23), the magnitude

and the phase of the main peak in each T -long section of the later signal. Then the associated symbols are decoded and the signal could be reproduced in each symbol section and subtracted from the received signal.

If we note $\hat{z}_s(n, p_s)$ the reconstruction of the synchronized signal, in the p_s^{th} T -long section, synthesized by the estimation of its frequency $\hat{m}_s(p_s)$, magnitude $\sqrt{\hat{P}_s^{p_s}}$ and initial phase $\hat{\phi}^{p_s}$, we have:

$$z(n, p_s) = z(n, p_s) - \hat{z}_s(n, p_s) \quad (24)$$

where $\hat{z}_s(n, p_s)$ is expressed as:

$$\hat{z}_s(n, p_s) = \sqrt{\hat{P}_s^{p_s}} e^{j(2\pi n \frac{\hat{m}_s(p_s)}{M} + \hat{\phi}^{p_s})} \quad (25)$$

In same context, authors in [12] proved that the SIC could be performed only if the power ratio between the strongest signal and the weak one is at least 1 dB.

D. Processing of superimposed peaks

Dealing with simultaneously received LoRa-like signals with the same SF causes some critical cases that should be studied to avoid the degradation of the decoding performance. As presented in (21), after the FFT processing, the synchronized signal contributes by one Dirac at the symbol to estimate, but the other existent signals contribute by two cardinal sines each. As a result, there is a non-null probability that one of these peaks is located at the same FFT bin with the Dirac of the synchronized signal. In this case, after estimating the frequency, magnitude and phase of the main peak, the latter is removed and then the contribution of the other existent signals in the same FFT bin is also reduced.

To address this issue, we propose to compare the magnitude of the current FFT main peak with a mean value, denoted $\sqrt{\bar{P}_s}$ and computed from the main peaks in all the T -long sections of the signal of interest. If this current magnitude is considerably greater than the mean value, two or more superposed peaks are assumed to be detected. In this case, an hypothesis test is done by referring to the distribution of the demodulation metric $|Y_s(k, p_s)|$. Thus, if we suppose that there are no interfering signals in the p_s^{th} T -long section and by using the basic properties of the complex normal distribution, we have:

$$|Y_s(k, p_s)| \sim \begin{cases} \mathcal{R}_i(\sqrt{P_s M}, \sigma_w) & \text{for } k = m_s(p_s) \\ \mathcal{R}_i(0, \sigma_w) & \text{else} \end{cases} \quad (26)$$

Where $\mathcal{R}_i(u, v)$ is the Rician distribution with u and v are the location and the scale parameters.

In this case, we define the hypothesis of our test as:

- \mathcal{H}_0 : one peak exists at the FFT bin of the symbol to be decoded.
- \mathcal{H}_1 : two or more peaks are superposed at the FFT bin of the symbol to be decoded.

Using the same definition of the probability of false alarm P'_{fa} as we detailed in IV-A1, we can easily deduce the value of the threshold allowing the detection of two or more peaks at the FFT bin of the symbol to be decoded:

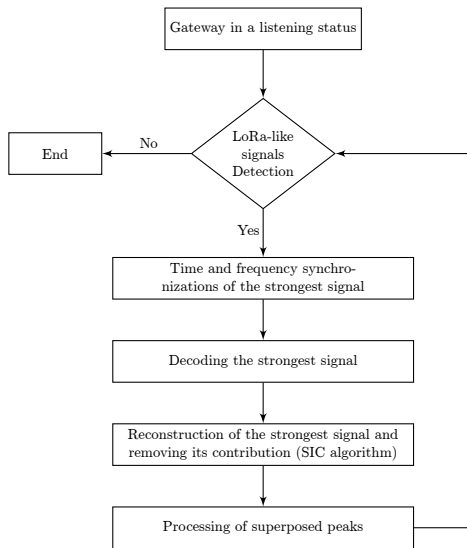


Fig. 8: Adopted algorithm.

$$Th' = F_{\mathcal{R}_i}^{-1}(1 - P'_{fa}; \sqrt{P_s M}, \sigma_w) \quad (27)$$

Once the receiver detects the presence of two or more peaks at the FFT bin of the current symbol of the synchronized signal, the magnitude and the phase of the reconstructed signal in (25) will be $\sqrt{P_s}$ and $\bar{\phi}$, where $\bar{\phi}$ is the mean phase computed from the initial phases in all the T -long sections. It should be noted here that LoRa modulation is a memoryless continuous phase modulation [15]. Thus, the initial phases are equal in all the T -long sections.

Thereby, this operation allows to maintain the contribution of the signals other than the strongest one in the same FFT bin.

Finally, as depicted in Fig. 8, which summarizes the adopted approach to design our receiver, the algorithms in IV-A, IV-B, IV-C and IV-D are repeated until no LoRa-like signal is detected in the considered block. Reader can find more details about our algorithm in the pseudo-code in the appendix.

In the next section, the performance of our receiver are evaluated through Matlab® simulation and real LoRa deployments.

V. RESULTS AND DISCUSSIONS

In this section, we aim to evaluate the performance of our receiver to synchronize and decode simultaneously received LoRa-like signals with the same SF . To this end, we propose to:

- perform Monte Carlo based simulations using synthesized LoRa-like signals,
- use own-made LoRa nodes and gateways to validate our results with real LoRa deployments.

A. Simulation results on synthesized signals

1) *Considered scenario*: The considered scenario consists in simultaneously receiving U LoRa-like signals at random arrival instants using the parameters in Table V. The packets are generated using our Matlab® simulator and have the

structure as presented in III-A. For the sake of simplicity, we assumed that the simulated receiver is aware of the packet and the preamble lengths.

TABLE V: Simulation parameters

Bandwidth (kHz)	125
Spreading Factor	{12; 9}
Frame length	$80 \times T$
Block length T_B	$200 \times T$
Preamble length N_p	8
Number of superposed signals U	{2; 3; 4}
Number of Monte Carlo iterations	10000

In the following, we define the power ratio between each two received signals:

$$(PR_{i,j})_{dB} = 10 \log_{10} \left(\frac{P_i}{P_j} \right), \quad i, j \in \{1, \dots, U\} \quad (28)$$

When sorting the received powers by decreasing order, we consider that the power ratio (dB) between two consecutive elements as being constant and equal to PR .

Furthermore, the frequency shifts $\Delta f_i, \forall i \in \{1, \dots, U\}$ are supposed uniformly distributed in $[-\Delta f_{max}, \Delta f_{max}]$. The highest frequency offset Δf_{max} is equal to $5\% \times F_s$, with $F_s = \frac{1}{T_s}$ is the sampling frequency⁵.

2) *Start of frame detection*: The first step that our receiver has to perform is the detection of the received LoRa-like packets and the identification of the effective start of the frames. Using the coarse and fine synchronization methods as described in IV-A, we obtained in Fig. 9 the following curves of the accurate detection probabilities of the start of the frame as function of the Signal to Noise Ratio (SNR). For each signal, the SNR is defined as:

$$SNR = \frac{P_i}{\sigma_w^2} \quad (29)$$

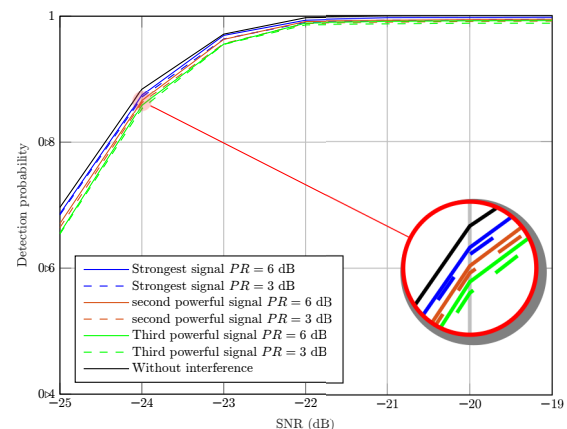


Fig. 9: Start of frame detection with $SF = 12$ and $U = 3$

Fig. 9 shows that, for $PR = 6$ dB and $PR = 3$ dB, the start of frame detection of all the received signals are slightly affected compared to the case of a single LoRa packet received

⁵ Δf_{max} has been chosen based on the local oscillators precision used for LPWAN applications.

without interference. These results prove the immunity of our detection and synchronization (time and frequency) methods against same- SF interference. In addition, a nearly optimal detection is reached for the SNRs greater than -22 dB. Thus, this detection method is consistent with deployment requirements of the LoRa technology which define the SNR threshold, as presented in Table IV, $\Gamma_{th}^{(12)} = -20$ dB.

3) *SIC performance*: To test the efficiency of our receiver to perfectly synchronize to the strongest signal and remove its contribution, we present in Fig. 10 the evolution of the de-chirped data block. Both spectrograms are obtained before performing the synchronization on the strongest signal in each iteration of our algorithm. Here we note that, in a synchronized mode, each de-chirped LoRa symbol gives constant frequency over the symbol time.

The spectrogram in Fig. 10a represents the initial de-chirped data block where the $U = 3$ preambles could be easily identified. We can observe the existence of 3 long temporal sequences having a constant frequency. Indeed, since the symbols of LoRa preamble have the same value, a constant frequency is obtained over N_p symbol times.

After iterating our algorithm twice, it can be seen in Fig. 10b, that the contribution of the two signals having the highest received powers are perfectly removed. Hence, our receiver performs accurate time and frequency synchronizations.

4) *Decoding performance*: To evaluate the decoding performance of our proposed receiver, we display, in Fig. 11 and Fig. 12, the BER evolution of three superposed signals, with PR of 6 dB and 3 dB respectively, as a function of the SNR relative to each received signal as depicted in (29). We note that each dashed curve in both figures represents the BER of a received signal when all steps of our algorithm are performed, except for the processing of superimposed peaks. It can be seen that the decoding performance are enhanced (red and green solid curves) when we implement our algorithm to process the latter critical case.

Furthermore, based on [9], the solid blue curves in both figures show that the decoding performance of the strongest signal is almost identical to the case where only one same- SF interfering signal having a received power ratio of 3 dB and 6 dB is met. This result is explained by the fact that the contribution of the second strongest signal interferes more on the decision of the strongest signal symbols. In addition, we notice that its SNR threshold value, in Fig. 11 (resp. Fig. 12) is increased by almost 1 dB (resp. 5.3 dB) compared to the absence of interference case.

Once the latter signal is decoded, its contribution is removed to process the remaining signals. The solid red curves show that the decoding performance of the second strongest signal is slightly affected by comparing with the BER of strongest one. But, if the SNR is greater than -20 dB (resp. -15 dB) in Fig 11 (resp. Fig. 12) the BER remains almost constant. These results are explained by:

- the errors that occur when decoding the strongest signal and removing its contribution,
- the issue of superimposed peaks which can not be totally solved,

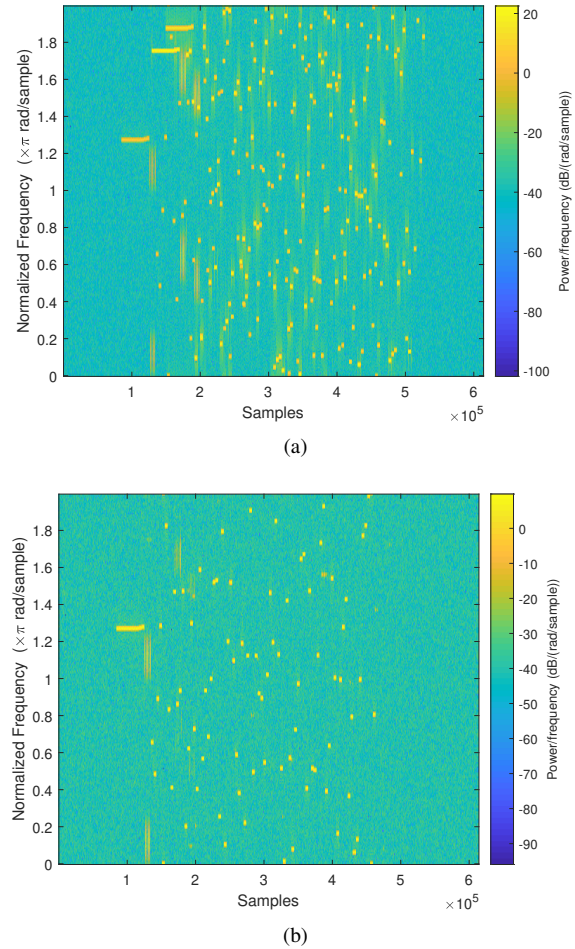


Fig. 10: Evolution of the de-chirped block with $PR = 3$ dB, $SF = 12$ and $U = 3$ - (a) initial state - (b) after two iterations.

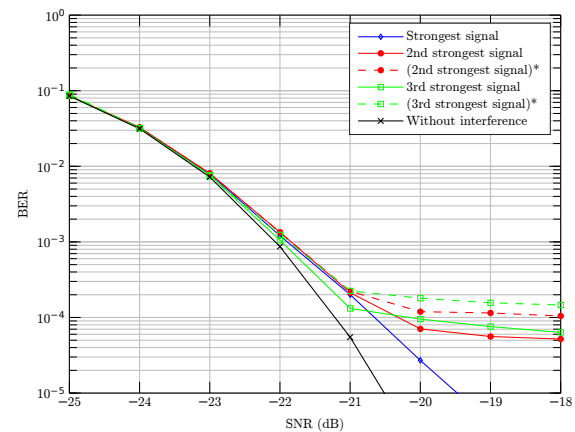


Fig. 11: BER evolution with $PR = 6$ dB, $SF = 12$ and $U = 3$

- the presence of the third strongest signal as an interfering signal with $PR = 6$ dB (resp. $PR = 3$ dB) in Fig. 11 (resp. Fig. 12).

Finally, the receiver has to process the remaining signal. The solid green curves show that the decoding performance of the weakest signal is slightly affected compared to the BER of one LoRa signal without interference. However, with a SNR = -20

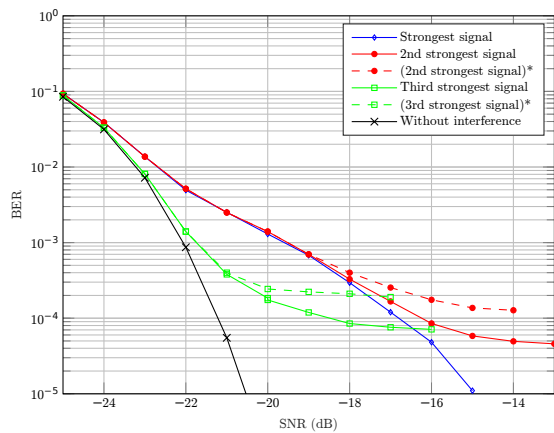


Fig. 12: BER evolution with $PR = 3$ dB, $SF = 12$ and $U = 3$

dB the BER remains almost constant. These results are also explained by the errors occurring when removing the previous signals. Nevertheless, in this case, the errors introduced by the SIC are more accentuated since two signals are already removed.

Based on the latter results, we can deduce that our receiver can decode accurately 3 superposed signals with $SF = 12$ if we guarantee 6 dB as a minimum power ratio between them.

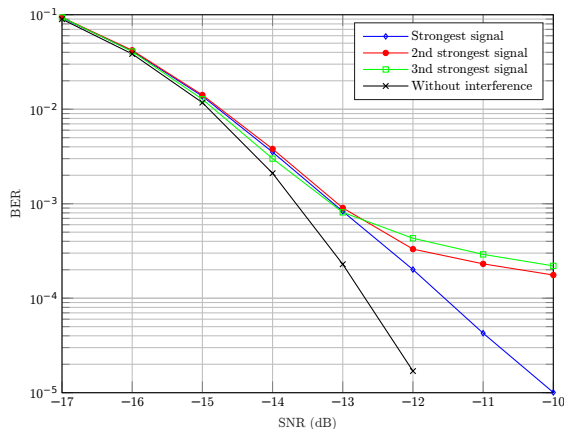


Fig. 13: BER evolution with $PR = 6$ dB, $SF = 9$ and $U = 3$.

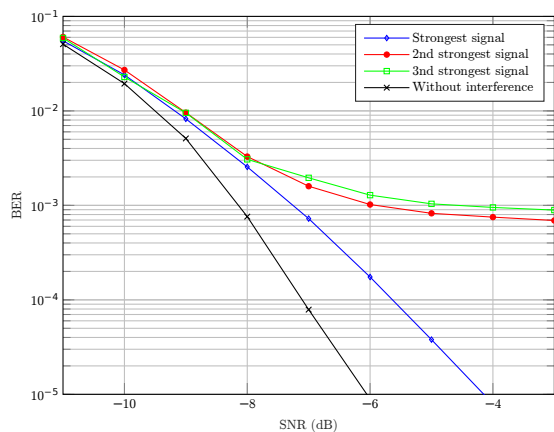


Fig. 14: BER evolution with $PR = 6$ dB, $SF = 7$ and $U = 3$.

In all the latter simulations, we used $SF = 12$ which has the longest time on air and is likely to involve collisions [24]. To show the impact of decreasing the SF on the decoding performance of our receiver, we represent in Fig. 13 the BER evolution of the received signals with $SF = 9$. It can be seen that we obtain almost the same results as in Fig. 11 with slightly degradation of the decoding performance of the second and the third received signals, which remain acceptable since a BER of 2×10^{-4} is reached at $SNR = 10$ dB for both signals. Similarly in Fig. 14, the latter performance degradation are more accentuated when the $U = 3$ superposed signals are received with $SF = 7$. Indeed, this degradation can be explained by the issue of superposed peaks which is more likely for the lowest SF since the number of points in the FFT is proportional to the SF .

Thus, our approach is more effective with the highest SF and allows to decode up to four simultaneously received signals as presented in the next simulation.

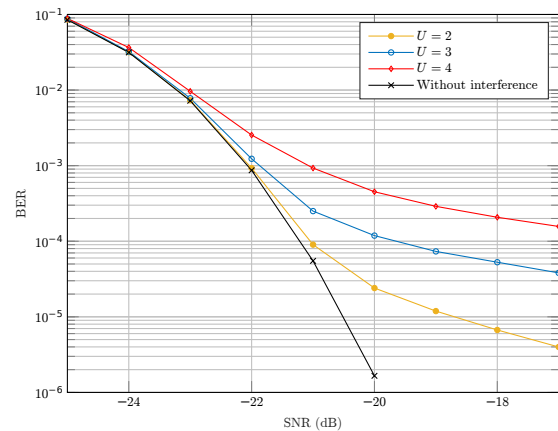


Fig. 15: BER evolution of the weakest signal with $SF = 12$.

The final simulation test is to evaluate the impact of increasing the number of superposed signals on the decoding performance of our receiver. To this end, we represent in Fig. 15 the BER evolution of the weakest received signal during T_B . Here, we assumed that PR is uniformly distributed in $[6, 10]$ dB. In such configuration, we notice that for $U = 2$ the weakest signal is effectively decoded since at the SNR threshold $\Gamma_{th}^{(SF=12)}$, the BER is equal to 2×10^{-5} . However, given that errors in decoding the synchronized signal are spread over the residual signals at each iteration, the decoding performance of the weakest signal are more degraded for $U \in \{3, 4\}$. Nevertheless, the latter performance remain acceptable since a BER of 10^{-4} is reached at $\Gamma_{th}^{(SF=12)}$ for $U = 3$ and a BER of 2×10^{-4} is reached for $U = 4$ at $SNR = -18$ dB.

B. Experimental validation

In this section, we aim to validate our simulation results by considering real LoRa deployments. To that end, we use own-made LoRa nodes and gateways as represented in Fig. 16 and detailed in [25].

Three LoRa nodes ($U = 3$) are configured to transmit continuously, with the same SF (here $SF = 12$), the same

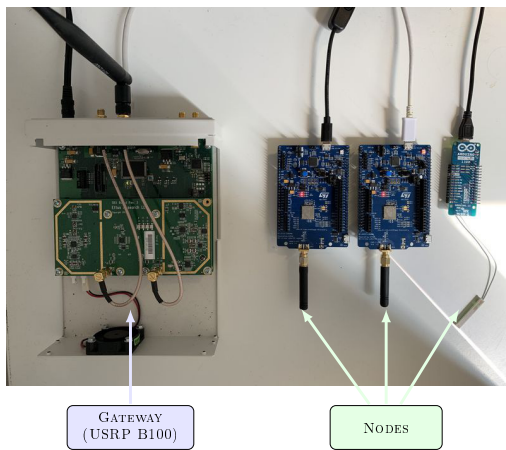


Fig. 16: Test-bed: Three LoRa node transmitting and one USRP SDR device receiving data.

message every second with a constant power ratio $PR = 6$ dB. Thus, high probability of collision between LoRa signals is obtained. All the nodes send data at a 868.2 MHz carrier frequency with a bandwidth $B = 125$ kHz. We also use Software Defined Radios (SDR) Universal Software Radio Peripheral (USRP) B100 [26] to acquire and process data.

In order to estimate the noise level detected by the receiver (i.e. compute σ_w^2), we start the acquisition on the reception side when the nodes are not transmitting. Then, we start the transmission of all the nodes randomly without any previous timing synchronization. To maintain the same power ratio between received signals as configured in the nodes, the latter are placed at the same distance from the USRP.

Fig. 17 presents the result of the FFT processing in a p^{th} T -long section, where $U_p = 3$. It represents the the capability of our receiver to synchronize on the strongest signal in each iteration and to remove its contribution to process the remaining signals.

The spectrum in Fig. 14a shows that, with real LoRa signals, it is difficult to obtain a perfect Dirac for the synchronized signal as in the theory. We also notice that this spectrum is consistent with (22), where each non synchronized signal contributes with two cardinal sines.

Furthermore, as we can see in Fig. 17b, the contribution of the strongest signal is not perfectly removed but dramatically reduced by 28 dB. This proves that our receiver efficiently performs time and frequency synchronizations and estimates accurately the frequency, the magnitude and the phase of the latter signal in each T -long section.

Once the contribution of the latter signal is removed, the receiver performs time and the frequency synchronizations on the signal having the second highest received power. In Fig. 17c, it can be seen that the power ratio between the latter two signals is 7 dB, which is almost equal to the power ratio configured on the transmitting nodes since they are equidistant to the USRP. In addition, removing the contribution of the synchronized signal by almost 28 dB provides a good margin to process the remaining ones.

Finally, thanks to our approach, we were able to synchronize (time and frequency synchronizations) and decode the signal

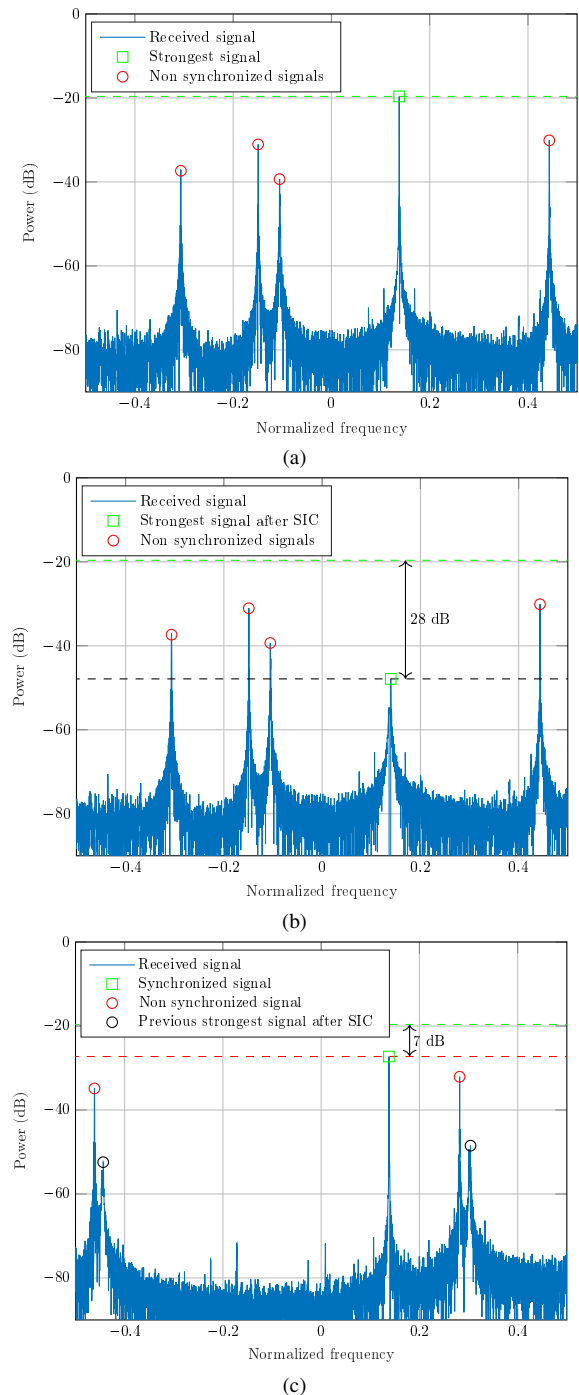


Fig. 17: Result of the FFT - (a) synchronization on the strongest signal - (b) strongest signal cancellation - (c) synchronization on the second strongest signal.

information from the 3 nodes. This interesting performance would increase considerably the capacity of LoRa technology-based networks, enhance the spectral efficiency and reduce the energy consumption of the nodes.

VI. CONCLUSION

With the exponential growth of the number of connected objects, packet collisions are becoming a challenge for the IoT systems. In LoRa communication, the use of RACH to avoid

the collisions is far from ideal. Therefore, in this paper, we propose the design of a receiver capable to process destructive LoRa-like collisions. Indeed, we showed through mathematical models, simulation results and experimental validation that simultaneously received LoRa-like signals with the same SF could be processed and we were able to extract the information from the transmitting nodes. As a result, our novel approach would reduce the energy consumption of the nodes and enhance the capacity of LoRa technology-based networks since it decreases the number of re-transmitted packets.

Our solution has also the advantage of using the commercialized LoRa chip to process collisions. Thus, it can be easily implemented to an existing network to enhance spectral efficiency. As future work, a complete link and system level simulator would be developed to outline the benefits of the proposed approach in a real-world scenario in terms of throughput and energy consumption. Indeed, same and different SF interference would be considered as well as interference from other technologies in ISM bands. Moreover, we are planning to enhance the processing for the lowest SF in order to deal with the issue of superposed peaks.

ACKNOWLEDGEMENT

The authors would like to thank F. LE NEINDRE and M. REZZOUKI for their insights and help on managing the USRP SDR devices and LoRa nodes.

REFERENCES

- [1] IoT Analytics GmbH, "State of the IoT and Short-term outlook," 2018. [Online]. Available: <https://iot-analytics.com/product/state-of-the-iot-2018/>
- [2] Semtech, "LoRa modem design guide: Sx1272/3/6/7/8," 2013. [Online]. Available: https://www.semtech.com/uploads/documents/LoraDesignGuide_STD.pdf
- [3] "Low power long range transmitter," Patent, Jan., 2014. [Online]. Available: <https://patents.google.com/patent/US20140219329A1/en>
- [4] L. Vangelista, "Frequency shift chirp modulation: The lora modulation," *IEEE Signal Processing Letters*, vol. 24, no. 12, pp. 1818–1821, Dec 2017.
- [5] B. Reynders and S. Pollin, "Chirp spread spectrum as a modulation technique for long range communication," in *2016 Symposium on Communications and Vehicular Technologies (SCVT)*, Nov 2016, pp. 1–5.
- [6] LoRa Alliance, "LoRaWAN® Specification v1.1," 2017. [Online]. Available: <https://lora-alliance.org/resource-hub/lorawanr-specification-v11>
- [7] M. Ni, M. Jafarizadeh, and R. Zheng, "On the effect of multi-packet reception on redundant gateways in lorawans," in *ICC 2019 - 2019 IEEE International Conference on Communications (ICC)*, May 2019, pp. 1–6.
- [8] T. Elshabrawy and J. Robert, "Analysis of BER and Coverage Performance of LoRa Modulation under Same Spreading Factor Interference," in *2018 IEEE 29th Annual International Symposium on Personal, Indoor and Mobile Radio Communications (PIMRC)*, Sep. 2018, pp. 1–6.
- [9] O. Afisiadis, M. Cotting, A. P. Burg, and A. Balatsoukas-Stimming, "Lora symbol error rate under non-chip- and non-phase-aligned interference," *ArXiv*, vol. abs/1905.00439, 2019.
- [10] D. Croce, M. Gucciardo, S. Mangione, G. Santaromita, and I. Tinnirello, "Impact of lora imperfect orthogonality: Analysis of link-level performance," *IEEE Communications Letters*, vol. 22, no. 4, pp. 796–799, April 2018.
- [11] J. Markkula, K. Mikhaylov, and J. Haapola, "Simulating lorawan: On importance of inter spreading factor interference and collision effect," in *ICC 2019 - 2019 IEEE International Conference on Communications (ICC)*, May 2019, pp. 1–7.
- [12] U. Noreen, L. Clavier, and A. Bounceur, "LoRa-like CSS-based PHY layer, Capture Effect and Serial Interference Cancellation," in *European Wireless 2018; 24th European Wireless Conference*, May 2018, pp. 1–6.
- [13] N. E. Rachkidy, A. Guitton, and M. Kaneko, "Decoding Superposed LoRa Signals," *CoRR*, vol. abs/1804.00503, 2018. [Online]. Available: <http://arxiv.org/abs/1804.00503>
- [14] B. Laporte-Fauret, M. A. Ben Temim, G. Ferré, D. Dallet, B. Minger, and L. Fuché, "An enhanced LoRa-Like receiver for the simultaneous reception of two interfering signals," in *2019 IEEE 30th Annual International Symposium on Personal, Indoor and Mobile Radio Communications (PIMRC)*, Sep. 2019.
- [15] M. Chiani and A. Elzanaty, "On the lora modulation for iot: Waveform properties and spectral analysis," *CoRR*, vol. abs/1906.04256, 2019. [Online]. Available: <http://arxiv.org/abs/1906.04256>
- [16] T. Elshabrawy and J. Robert, "Interleaved chirp spreading lora-based modulation," *IEEE Internet of Things Journal*, vol. 6, no. 2, pp. 3855–3863, April 2019.
- [17] R. Ghanaatian, O. Afisiadis, M. Cotting, and A. Burg, "Lora digital receiver analysis and implementation," *CoRR*, vol. abs/1811.04146, 2018. [Online]. Available: <http://arxiv.org/abs/1811.04146>
- [18] V. Talla, M. Hesar, B. Kellogg, A. Najafi, J. R. Smith, and S. Gollakota, "Lora backscatter: Enabling the vision of ubiquitous connectivity," *Proc. ACM Interact. Mob. Wearable Ubiquitous Technol.*, vol. 1, no. 3, pp. 105:1–105:24, Sep. 2017. [Online]. Available: <http://doi.acm.org/10.1145/3130970>
- [19] J. C. Liando, A. Gamage, A. W. Tengourtius, and M. Li, "Known and unknown facts of lora: Experiences from a large-scale measurement study," *ACM Trans. Sen. Netw.*, vol. 15, no. 2, pp. 16:1–16:35, Feb. 2019. [Online]. Available: <http://doi.acm.org/10.1145/3293534>
- [20] "Communication Systems," Patent, Jan., 2016. [Online]. Available: <https://patents.google.com/patent/EP2449690B1/en>
- [21] G. Colavolpe, T. Foggi, M. Ricciulli, Y. Zanettini, and J. Mediano-Alameda, "Reception of lora signals from leo satellites," *IEEE Transactions on Aerospace and Electronic Systems*, pp. 1–1, 2019.
- [22] G. Ferré and A. Giremus, "LoRa Physical Layer Principle and Performance Analysis," in *2018 25th IEEE International Conference on Electronics, Circuits and Systems (ICECS)*, Dec 2018, pp. 65–68.
- [23] M. Knight and B. Seeber, "Decoding lora: Realizing a modern lpwan with sdr," *Proceedings of the GNU Radio Conference*, vol. 1, no. 1, 2016. [Online]. Available: <https://pubs.gnuradio.org/index.php/grcon/article/view/8>
- [24] G. Ferré and E. P. Simon, "Packet collision analysis when heterogeneous unlicensed IoT technologies coexist," *IET Networks*, May 2018. [Online]. Available: <http://digital-library.theiet.org/content/journals/10.1049/iet-net.2018.0026>
- [25] G. Ferré, F. Rivet, R. Tajan, and E. Kerhervé, "Design and Deployment of an IoT Network Based on LoRa," in *EAEEIE (European Association for Education in Electrical and Information Engineering)*, Grenoble, France, Jun. 2017.
- [26] Ettus Knowledge Base, "B100 — Ettus Knowledge Base," 2016. [Online]. Available: <https://kb.ettus.com/index.php?title=B100&oldid=2983>

APPENDIX

Algorithm 1: Decoding superposed LoRa-like signals

Input: $y(n)$, SF , B , N_B
 $M \leftarrow 2^{SF}$.
 $z(n, p) \leftarrow (13)$, $n \in \llbracket pM, (p+1)M - 1 \rrbracket$ and
 $p \in \{1, \dots, N_B\}$ (dechirping operation).
 $Y(k, p) \leftarrow (12)$, $k \in \llbracket 0, M - 1 \rrbracket$ (FFT).
 $T(k, p) \leftarrow (15)$ (averaging function).
 $M(p) \leftarrow \max_k(T(k, p))$.
 $Th \leftarrow (19)$ (noise threshold).
while $\exists p \in \{1, \dots, N_B\}, M(p) > Th$ **do**
 $\hat{K}_s \leftarrow \underset{p}{\operatorname{argmax}}(M(p))$.
 $\hat{\tau}_s, \hat{\Delta}f_s \leftarrow$ fine synchronization (section IV-A2).
 $\Delta n_s \leftarrow \hat{K}_s M + \hat{\tau}_s$.
 for $p_s \leftarrow 1$ to N_{symbols} **do**
 $z_s(n, p_s) \leftarrow (21)$,
 $n \in \llbracket \Delta n_s + p_s M, \Delta n_s + (p_s + 1)M - 1 \rrbracket$.
 $Y^s(k, p_s) \leftarrow FFT(z_s(n, p_s))$.
 $\hat{m}_s(p_s) \leftarrow \underset{k}{\operatorname{argmax}}(|Y^s(k, p_s)|)$ (estimated
 symbol).
 $\sqrt{\hat{P}_s^{p_s}} \leftarrow \max_k(|Y^s(k, p_s)|)$ (estimated
 magnitude).
 $\hat{\phi}^{p_s} \leftarrow \arg(|Y^s(\hat{m}_s(p_s), p_s)|)$ (estimated
 phase).
 $Th' \leftarrow (27)$ (threshold to detect superposed
 signals).
 if $\sqrt{\hat{P}_s^{p_s}} > Th'$ **then**
 $\hat{A}_r \leftarrow \underset{p_s}{\operatorname{mean}}(\sqrt{\hat{P}_s^{p_s}})$.
 $\hat{\phi}_r \leftarrow \underset{p_s}{\operatorname{mean}}(\hat{\phi}^{p_s})$
 else
 $\hat{A}_r \leftarrow \sqrt{\hat{P}_s^{p_s}}$.
 $\hat{\phi}_r \leftarrow \hat{\phi}^{p_s}$.
 end
 $\hat{z}_s(n, p_s) \leftarrow \hat{A}_r e^{j(2\pi n \frac{\hat{m}_s(p_s)}{M} + \hat{\phi}_r)}$
 (reconstruction of the strongest signal).
 $z(n, p_s) \leftarrow z(n, p_s) - \hat{z}_s(n, p_s)$ (SIC).
 end
 $T(k, p) \leftarrow (15)$.
 $M(p) \leftarrow \max_k(T(k, p))$.
end
